Talk IV: Flat 2-torus in $\mathbb{E}^3$

Vincent Borrelli

January 6, 2014

In the previous document we gave a general description of a convex integration process which is appropriate for the Nash-Kuiper construction of isometric embeddings. Here we specify this process to the case of isometric embeddings of a square flat torus in $\mathbb{E}^3$. We then discuss the geometric structure of their images.

1 Isometric embeddings of square flat tori in $\mathbb{E}^3$

Definition.– A *flat torus* is a quotient $\mathbb{E}^2/\Lambda$ where $\Lambda = \mathbb{Z}U \oplus \mathbb{Z}V \subset \mathbb{E}^2$ is a lattice. This quotient is called a *square flat torus* if it is isometric to a quotient $\mathbb{E}^2/\mathbb{Z}U_1 \oplus \mathbb{Z}V_1 \subset \mathbb{E}^2$ where (U_1, V_1) is an orthonormal basis of $\mathbb{E}^2$.

Exemple.– Let (e_1, e_2) be an orthonormal basis of $\mathbb{E}^2$. The quotients $\mathbb{E}^2/\mathbb{Z}U(i) \oplus \mathbb{Z}V(i)$, $i \in \{1, 2, 3\}$ with

$$\begin{array}{lll} U(1) = e_1 & U(2) = \frac{1}{5}(e_1 + 2e_2) & U(3) = \frac{1}{5}(e_1 - 2e_2) \\ V(1) = e_2 & V(2) = -2e_1 + e_2 & V(3) = 2e_1 + e_2 \end{array}$$

define the same square flat torus (up to isometries). We denote by $\mathbb{T}^2$ this square flat torus and by Dom_i the fundamental domain spanned by $U(i)$ and $V(i)$.

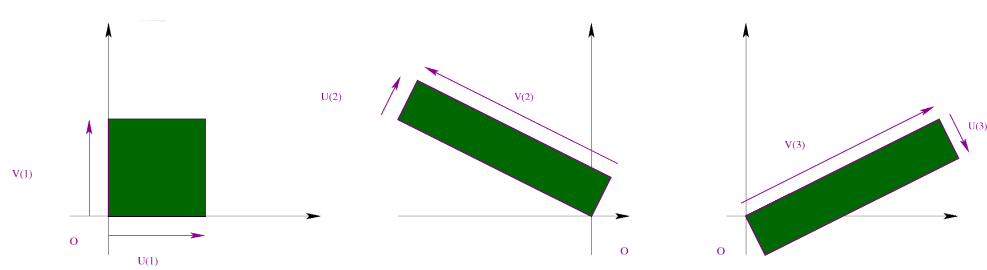

Three fundamental domains Dom_i, $i \in \{1, 2, 3\}$, of the same square flat torus $\mathbb{T}^2$.

Lemma.– *Let $R > r > 0$ and*

$$
\begin{array}{rccc}
f_0: & \mathbb{T}^2 = \mathbb{E}^2/\mathbb{Z}e_1 \oplus \mathbb{Z}e_2 & \longrightarrow & \mathbb{E}^3 \\
 & (u,v) & \longmapsto & \left\{ \begin{array}{l} \frac{1}{2\pi}(R + r\cos 2\pi u)\cos 2\pi v \\ \frac{1}{2\pi}(R + r\cos 2\pi u)\sin 2\pi v \\ \frac{r}{2\pi}\sin 2\pi u \end{array} \right.
\end{array}
$$

If $R + r < 1$ then f_0 is a strictly short embedding of $\mathbb{T}^2$ in $\mathbb{E}^3$.

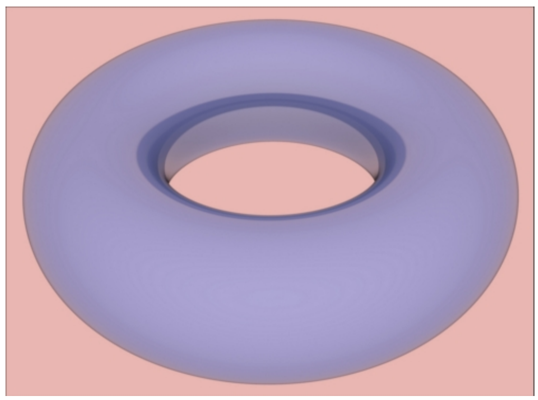

The image of $\mathbb{T}^2$ by f_0.

Proof.– A straightforward computation shows that

$$f_0^*\langle .,. \rangle_{\mathbb{E}^3} = r^2 du^2 + (R + r\cos 2\pi u)^2 dv^2.$$

Therefore $f_0^*\langle .,. \rangle_{\mathbb{E}^3} < du^2 + dv^2$ iff $R + r < 1$. $\square$

Let us choose f_0 as initial map. The image of its isometric default

$$
\begin{array}{rccc}
\Delta: & \mathbb{T}^2 & \longrightarrow & \mathcal{M} \\
 & (u,v) & \longmapsto & (1 - r^2)du^2 + (1 - R - r\cos 2\pi u)^2 dv^2
\end{array}
$$

is a segment lying inside the positive cone of inner products

$$\mathcal{M} = \{Edu^2 + 2Fdudv + Gdv^2 \mid E > 0, EG - F^2 > 0\}$$

of $\mathbb{E}^2$.

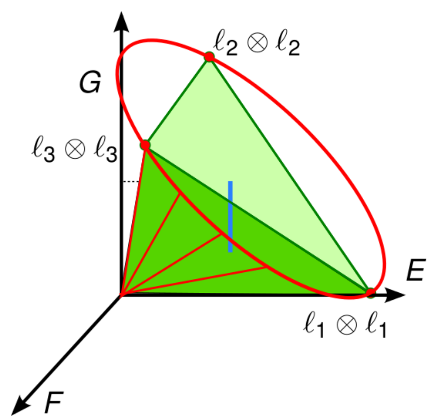

The image of the isometric default Δ is the blue segment, the positive cone of inner products is pictured in red.

Let ℓ_1, ℓ_2 and ℓ_3 be the three linear form of $\mathbb{E}^2$ defined by

$$\forall\, i \in \{1,2,3\}, \quad \ell_i(.) = \Big\langle \frac{U(i)}{\|U(i)\|_{\mathbb{E}^2}}, . \Big\rangle_{\mathbb{E}_2}$$

where the $U(i)$s are the ones appearing in the above exemple. It is easily checked that $\Delta(\mathbb{T}^2)$ lies inside the positive cone spanned by the $\ell_i \otimes \ell_i$. Therefore there exist three positive functions ρ_1, ρ_2 and ρ_3 such that

$$\Delta = \rho_1 \ell_1 \otimes \ell_1 + \rho_2 \ell_2 \otimes \ell_2 + \rho_3 \ell_3 \otimes \ell_3.$$

We are now in position to apply the general process described in the previous document in order to iteratively construct an isometric embedding. It turns out that we can manage to keep the same set of three linear forms $\{\ell_1, \ell_2, \ell_3\}$ during all the process (that point won't be detailed here) therefore we are going to obtain a sequence

$$f_0, \qquad f_{1,1}, f_{1,2}, f_{1,3}, \qquad f_{2,1}, f_{2,2}, f_{2,3}, \quad etc.$$

Each map $f_{k,j}$ is built from $f_{k,j-1}$ by a convex integration over the domain Dom_j (we use the circular convention $f_{k,0} := f_{k-1,3}$).

Let us see the details of the construction of $f_{k,1}$ from the map $f_{k,0}$. The isometric default of $f_{k,0}$ is

$$g_k - f_{k,0}^* \langle ., \rangle_{\mathbb{E}^3} = \rho_{k,1} \ell_1 \otimes \ell_1 + \rho_{k,2} \ell_2 \otimes \ell_2 + \rho_{k,3} \ell_3 \otimes \ell_3.$$

Recall that we want $f_{k,1}$ to have an isometric default roughly equal to the sum of the last two terms $\rho_{k,2}\ell_21 \otimes \ell_2 + \rho_{k,3}\ell_3 \otimes \ell_3$. To this end we introduce the intermediary metric

$$\mu_{k,1} := f_{k,0}^*\langle ., . \rangle_{\mathbb{E}^3} + \rho_{k,1}\ell_1 \otimes \ell_1$$

and observe that the above requirement amounts to ask that $f_{k,1}$ is quasi-isometric for $\mu_{k,1}$. Let

$$W_{k,1} := U(1) + \zeta_{k,1}V(1)$$

with

$$\zeta_{k,1} = -\frac{(f_{k,0}^*\langle ., . \rangle_{\mathbb{E}^3})(U(1), V(1))}{(f_{k,0}^*\langle ., . \rangle_{\mathbb{E}^3})(V(1), V(1))}.$$

The vector field $W_{k,1}$ is orthogonal to the field $V(1)$ for the metric $\mu_{k,1}$ and its integral curves $\varphi(., c)$ of issuing from the line $\mathbb{R}V(1)$ of Dom_1 define a diffeomorphism $\varphi : \mathbb{R}/\mathbb{Z} \times [0, 1] \to (\mathbb{R}/\mathbb{Z})V(1) \times [0, 1]U(1)$.

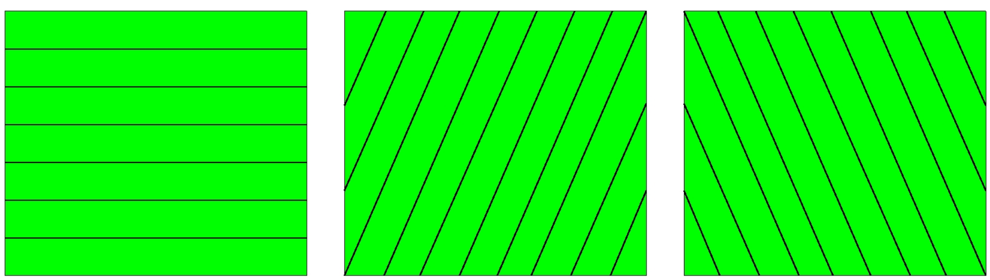

The integral lines of $W_{k,j}$ with $j = 1$, 2 and 3.

We now build a new map $F_{k,1}$ by applying to $f_{k,0}$ a two-dimensional convex integration along the integral curves $\varphi(., c)$, *i.e.*,

$$F_{k,1}(\varphi(s, c)) := f_{k,0}(0, c) + \int_0^s r(\varphi(u, c))\mathbf{e}^{i\theta(\varphi(u,c),u)}\mathrm{d}u$$

with $r = \sqrt{\mu_{k,1}(W_{k,1}, W_{k,1})}$, $\theta(q, u) := \alpha(q)\cos 2\pi N_{k,1}u$, $\alpha = J_0^{-1}\left(\frac{\|df_{k,0}(W_{k,1})\|}{r}\right)$, $\mathbf{t} = \frac{df_{k,0}(W_{k,1})}{\|df_{k,0}(W_{k,1})\|}$, $\mathbf{n}$ is a unit normal to the surface and $N_{k,1}$ is the number of corrugations.

Note that the map $F_{k,1}$ is properly defined over a cylinder, but does not descend to the torus in general. We eventually glue the two cylinder boundaries with the following formula, leading to a map $f_{k,1}$ defined over $\mathbb{T}^2 = \mathbb{E}^2/\mathbb{Z}^2$:

$$f_{k,1} \circ \varphi(s,c) := F_{k,1} \circ \varphi(s,c) - w(s).(F_{k,1} - f_{k,0}) \circ \varphi(1,c)$$

where $w : (0,1) \to (0,1)$ is a smooth S-shaped function satisfying $w(0) = 0$, $w(1) = 1$ and $w^{(k)}(0) = w^{(k)}(1) = 0$ for all $k \in \mathbb{N}^*$.

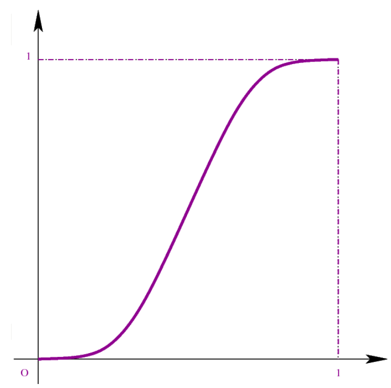

The function w.

Let $c' \in [0,1]$ such that $\varphi(1,c) = (1,c')$. We have

$$f_{k,0} \circ \varphi(1,c) = f_{k,0}(1,c') = f_{k,0}(0,c') = F_{k,1}(0,c').$$

Hence, in the above formula defining $f_{k,1}$, the difference

$$(F_{k,1} - f_{k,0}) \circ \varphi(1,c) = F_{k,1}(1,c') - F_{k,1}(0,c')$$

is precisely the gap that prevent $F_{k,1}$ to descend to the quotient.

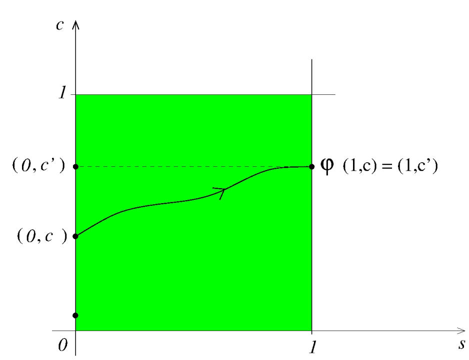

A flow line with endpoints $(0,c)$ and $\varphi(1,c) = (1,c')$.

In order to cancel the last two terms $\rho_{k,2}\ell_2 1 \otimes \ell_2 + \rho_{k,3}\ell_3 \otimes \ell_3$ in the isometric default, we apply two more corrugations in a similar way. For every j, the intermediary metric $\mu_{k,j}$ involves $f_{k,j-1}$ and the jth coefficient of the isometric default $g_k - f^*_{k,j-1}\langle .,. \rangle_{\mathbb{E}^3}$. Notice that the three resulting maps $f_{k,1}$, $f_{k,2}$ and $f_{k,3}$ are completely determined by their numbers of corrugations $N_{k,1}$, $N_{k,2}$ and $N_{k,3}$.

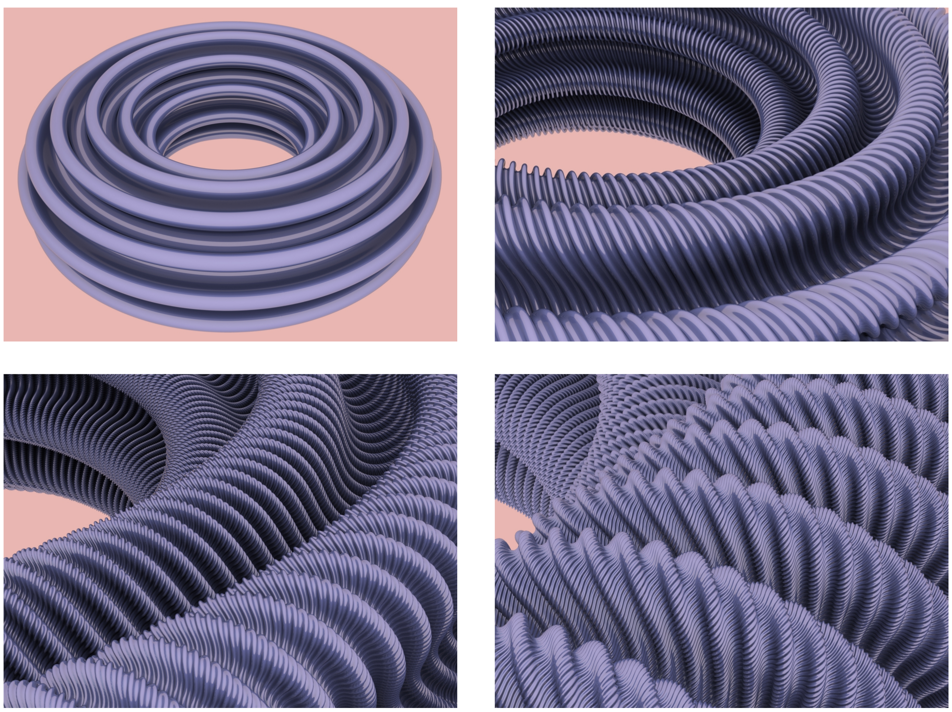

Images of the maps $f_{1,1}$, $f_{1,2}$, $f_{1,3}$ and $f_{2,1}$.

For the implementation, we choose the following sequence of metrics converging toward $\langle .,. \rangle_{\mathbb{E}^2}$:

$$g_k := f_0^* \langle \cdot, \cdot \rangle_{E^q} + \delta_k \Delta$$

with $\delta_k = 1 - e^{-k\gamma}$ and $\gamma = 0.1$. We also take $R = \frac{1}{4\pi}$ and $r = \frac{1}{10\pi}$ in the definition of f_0. The number of corrugations of the four first maps are 12, 80, 500, and 9,000. A grid of 2 milliards nodes was needed to picture the image of the fourth map. The visualization of the map $f_{2,1}$ shows that the image of the limit map f_∞ has a geometric structure which looks like a fractal.

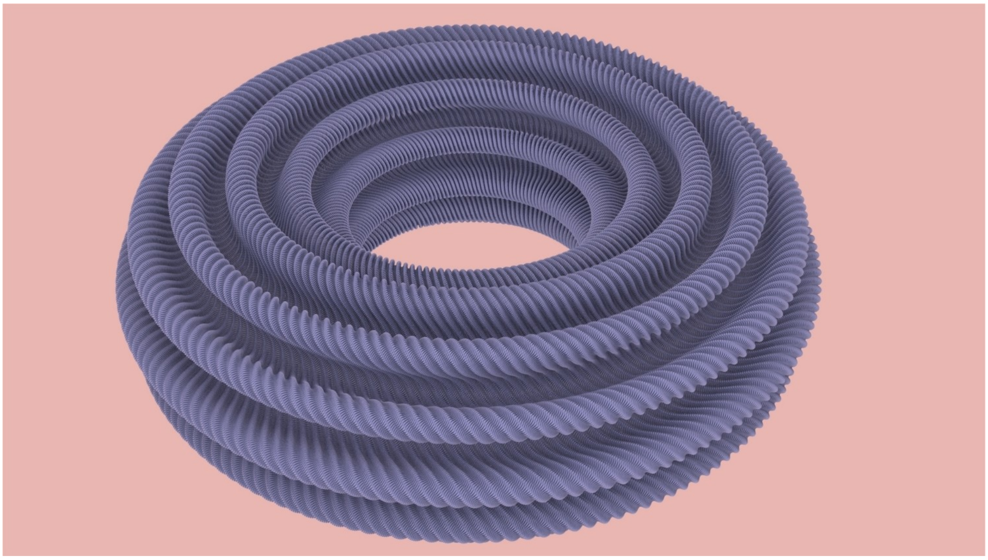

The image of $f_{2,1}$. Notice that the pointwise displacement between the map $f_{2,1}$ and the limit isometric map f_∞ could hardly be detected as the amplitude of each corrugation decreases dramatically. Further corrugations would thus not be visible to the naked eye.

Observation.– A numerical exploration seems to suggest that the growth of the number of corrugations is (at least) exponentional. This is in accordance with [2].

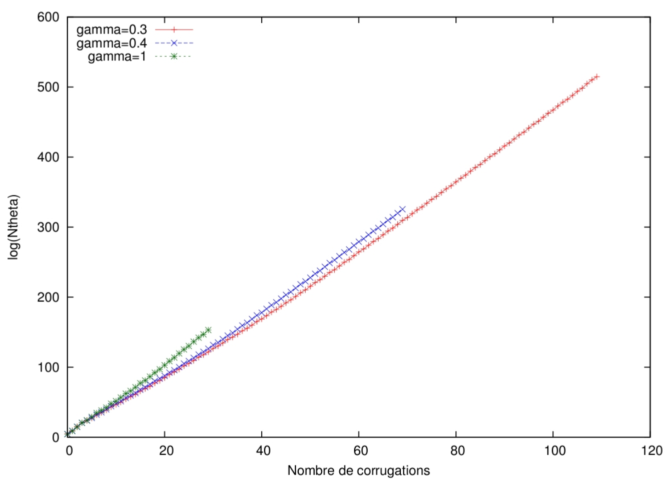

The growth of the N_k for various values of γ.

2 The convex integration process for curves

In that section we study the geometry of the image of limit map image in a one-dimensional setting. Precisely, we apply the convex integration process to a short curve of $\mathbb{E}^2$ and we set a explicite formula for the normal map of the limit curve. We then perform a Fourier decomposition of that normal map.

To simplify the computations, we assume that the inial short embedding $f_0 : \mathbb{S}^1 = \mathbb{E}/\mathbb{Z} \to \mathbb{E}^2$ is:

- $(Cond\ 1)$ of constant arc length
- $(Cond\ 2)$ radially symetric that is: $\frac{\partial f_0}{\partial x}(x + \frac{1}{2}) = -\frac{\partial f_0}{\partial x}(x)$.

Then the isometric default $\Delta := \langle ., . \rangle_{\mathbb{E}^2} - f_0^* \langle ., . \rangle_{\mathbb{E}^3}$ is constant and each metric $g_k := f_0^* \langle ., . \rangle_{\mathbb{E}^3} + \delta_k \Delta$ is also constant.

Proposition.– *Let $(N_k)_{k \in \mathbb{N}^*}$ be any sequence of natural even integers and $f_0 : \mathbb{S}^1 = \mathbb{E}/\mathbb{Z} \to \mathbb{E}^2$ be a short embedding satisfying conditions $(Cond\ 1)$ and $(Cond\ 2)$. For every $k \in \mathbb{N}^*$, let $f_k : ([0,1], g_k) \to \mathbb{E}^2$ be defined inductively by*

$$f_k(x) := f_{k-1}(0) + \int_0^x r_k \mathbf{e}^{i\alpha_k \cos 2\pi N_k s} \mathrm{d}s.$$

Then f_k descends to a isometry $f_k : (\mathbb{E}/\mathbb{Z}, g_k) \to \mathbb{E}^2$ which is short for g_{k+1} and which satisfies $(Cond\ 1)$ and $(Cond\ 2)$.

Remark.– As usual $r_k = \sqrt{g_k(\partial_x, \partial_x)}$, $\alpha_k = J_0^{-1}\left(\frac{\|f'_{k-1}\|}{r_k}\right)$, $\mathbf{e}^{i\theta} = \cos\theta\, \mathbf{t}_{k-1} + \sin\theta\, \mathbf{n}_{k-1}$, $\mathbf{t}_{k-1} = \frac{f'_{k-1}}{\|f'_{k-1}\|}$ and $\mathbf{n}_{k-1} = i\mathbf{t}_{k-1}$.

Proof.– By induction. Note that r_k is constant since g_k is constant. Since we have $\|\frac{\partial f_k}{\partial x}(x)\|^2_{\mathbb{E}^2} = r_k$, f_k satisfies $(Cond\ 1)$. Since, by induction hypothesis f_{k-1} satisfies $(Cond\ 1)$, the function α_k is constant. We have

$$\int_0^1 r_k \mathbf{e}^{i\alpha_k \cos 2\pi N_k s} \mathrm{d}s = 0$$

because N_k is even and f_{k-1} is radially symetric. Thus f_k descend to the quotient. It is trivial to check that f_k is also radially symetric. $\square$.

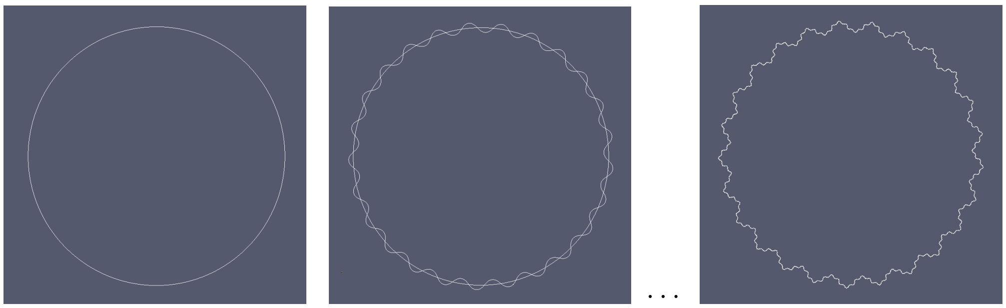

The convex integration process applied to circle

Let $(A_k)_{k\in N^*}$ be the sequence of functions defined by

$$\forall x \in \mathbb{S}^1, \quad A_k(x) := \sum_{l=1}^{k} \alpha_l \cos(2\pi N_l x).$$

Lemma.– *We have:*

$$\frac{\partial f_k}{\partial x}(x) = e^{iA_k(x)} \frac{r_k}{r_0} \frac{\partial f_0}{\partial x}(x).$$

Proof.– From

$$\begin{aligned} \frac{\partial f_k}{\partial x}(x) &= r_k(\cos(\alpha_k \cos(2\pi N_k x))\mathbf{t}_{k-1}(x) + \sin(\alpha_k \cos(2\pi N_k x))\mathbf{n}_{k-1}(x)) \\ &= r_k e^{i\alpha_k \cos(2\pi N_k x)} \frac{1}{r_{k-1}} \frac{\partial f_{k-1}}{\partial x}(x) \end{aligned}$$

we deduce by induction

$$\frac{\partial f_k}{\partial x}(x) = e^{iA_k(x)} \frac{r_k}{r_0} \frac{\partial f_0}{\partial x}(x).$$

$\square$

Warning.– We now assume that the sequence $(f_k)_{k\in\mathbb{N}}$ is C^1 converging toward its limit f_∞ and we set

$$\forall x \in \mathbb{E}/\mathbb{Z}, \quad A_\infty(x) := \sum_{l=1}^{+\infty} \alpha_l \cos(2\pi N_l x).$$

Corollary.– *The normal map $\mathbf{n}_\infty$ of f_∞ has the following expression*

$$\forall x \in \mathbb{E}/\mathbb{Z}, \quad \mathbf{n}_\infty(x) = e^{iA_\infty(x)}\mathbf{n}_0(x)$$

The formal expression of the normal map

$$\mathbf{n}_\infty(x) = \left(\prod_{l=1}^{+\infty} e^{i\alpha_l \cos(2\pi N_l x)}\right) \mathbf{n}_0(x)$$

is reminiscent of a *Riesz product.* These are products of the form

$$h(x) = \prod_{l=1}^{+\infty} (1 + \alpha_l \cos(2\pi N_l x)).$$

It is a fact that an exponential growth of N_l, known as Hadamard's lacunary condition, results in a fractional Hausdorff dimension of the Riesz measure[1] $\mu := h(x)\mathrm{d}x$ [3].

Lemma (Fourier Decomposition of n_k).– *Let $N_k := b^k$. For all $k \in \mathbb{N}$ we denotes by*

$$\forall x \in \mathbb{R}/\mathbb{Z}, \quad \mathbf{n}_k(x) := \sum_{p\in\mathbb{Z}} a_p(k) e^{2i\pi p x}$$

the Fourier decomposition of $\mathbf{n}_k$. Then

$$\forall p \in \mathbb{Z}, \quad a_p(k) = \sum_{n\in\mathbb{Z}} u_n(k) a_{p-nb^k}(k-1)$$

where $u_n(k) = i^n J_n(\alpha_k)$ (J_n denotes the Bessel function of order n).

Remark.– This formula gives the key to understand the construction of the spectrum $(a_p(k))_{p\in\mathbb{Z}}$ from the spectrum $(a_p(k-1))_{p\in\mathbb{Z}}$. The k-th spectrum is obtained by collecting an infinite number of shifts of the former spectrum. The n-th shift is of amplitude nb^{k-1} and weighted by $u_n(k) = i^n J_n(\alpha_k)$. Since

$$|J_n(\alpha_k)| \downarrow 0$$

the weight is decreasing with n.

[1] Let $dim_{\sup}\mu$ (resp. $dim_{\inf}\mu$) denotes the supremum (resp. the infimum) of the Hausdorff dimension of the Borel sets of positive μ-measure. If $d = dim_{\sup}\mu = dim_{\inf}\mu$ then the measure μ is said to have Hausdorff dimension d.

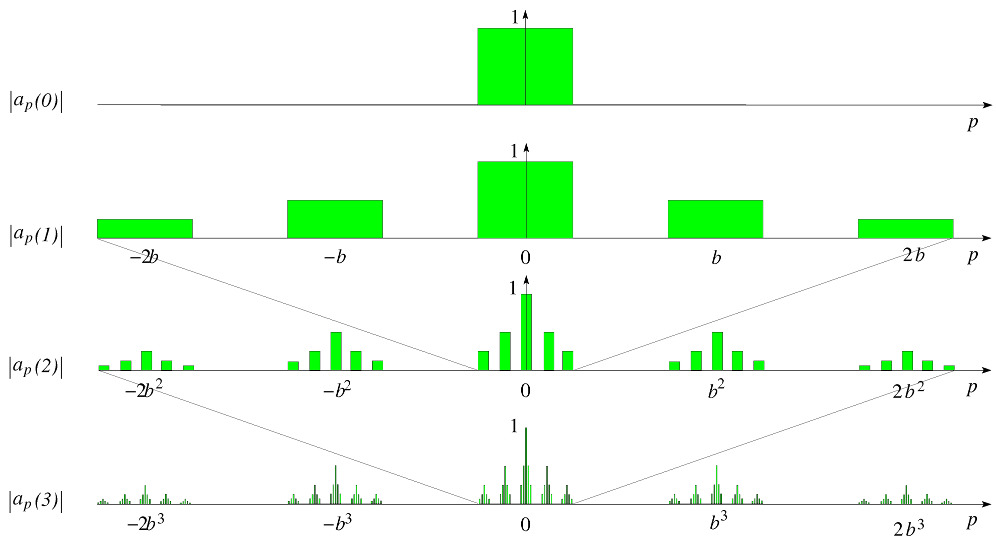

A schematic picture of the various spectra $(a_p(k))_{p\in\mathbb{Z}}$.

Proof of the Lemma.– From the Jacobi-Anger identity

$$e^{iz\cos\theta} = \sum_{n=-\infty}^{+\infty} i^n J_n(z) e^{in\theta}$$

we deduce

$$\begin{aligned} e^{i\alpha_k\cos(2\pi N_k x)} &= \sum_{n=-\infty}^{+\infty} i^n J_n(\alpha_k) e^{2i\pi n N_k x} \\ &= \sum_{n=-\infty}^{+\infty} u_n(k) e^{2i\pi n N_k x}. \end{aligned}$$

Since

$$\mathbf{n}_k(x) = e^{i\alpha_k\cos(2\pi N_k x)}\mathbf{n}_{k-1}(x)$$

we thus have

$$\begin{aligned} \mathbf{n}_k(x) &= \left(\sum_{n=-\infty}^{+\infty} u_n(k) e^{2i\pi n b^k x}\right)\left(\sum_{p=-\infty}^{+\infty} a_p(k-1) e^{2i\pi p x}\right) \\ &= \sum_{p=-\infty}^{+\infty}\left(\sum_{n=-\infty}^{+\infty} u_n(k) a_{p-nb^k}(k-1)\right) e^{2i\pi p x}. \end{aligned}$$

Therefore

$$a_p(k) = \sum_{n=-\infty}^{+\infty} u_n(k) a_{p-nb^k}(k-1). \qquad \square$$

3 Riesz-like fractal structure for flat tori

We now turn back to the case of the square flat torus. Previously, we have recursively built a sequence of embeddings $(f_{k,j})_{k\in\mathbb{N}^*, j\in\{1,2,3\}}$ converging toward a isometric embedding f_∞. Since this embedding is C^1 and not C^2, its geometry consists merely of the behavior of its tangent planes or, equivalently, of the properties of its *Gauss map*

$$\mathbf{n}_\infty : \mathbb{E}^2/\mathbb{Z}^2 \longrightarrow \mathbb{S}^2(1) \subset \mathbb{E}^3.$$

We denote by $\mathbf{v}_{k,j}$ the normalized derivative of $f_{k,j}$ in the direction $V(j)$ and by $\mathbf{n}_{k,j}$ the unit normal to $f_{k,j}$. We also set $\mathbf{v}^\perp_{k,j} := \mathbf{v}_{k,j} \times \mathbf{n}_{k,j}$. Obviously, there exists a matrix $\mathcal{C}_{k,j} \in SO(3)$ such that

$$(\mathbf{v}^\perp_{k,j} \quad \mathbf{v}_{k,j} \quad \mathbf{n}_{k,j})^t = \mathcal{C}_{k,j} \cdot (\mathbf{v}^\perp_{k,j-1} \quad \mathbf{v}_{k,j-1} \quad \mathbf{n}_{k,j-1})^t.$$

Here, $(\mathbf{a} \quad \mathbf{b} \quad \mathbf{c})^t$ stands for the transpose of the matrix with column vectors $\mathbf{a}, \mathbf{b}$ and $\mathbf{c}$. We call $\mathcal{C}_{k,j}$ a *corrugation matrix* since it encodes the effect of one corrugation on the map $f_{k,j-1}$. Note that the above formula is analogous to the formula

$$\mathbf{n}_k(x) = e^{i\alpha_k \cos(2\pi N_k x)} \mathbf{n}_{k-1}(x)$$

arising in the curves case. In particular, the Gauss map $\mathbf{n}_\infty$ of the limit embedding f_∞ can be expressed very simply by means of the corrugation matrices:

$$\forall k \in \mathbb{N}^*,\ \mathbf{n}^t_\infty = (0 \quad 0 \quad 1) \cdot \prod_{\ell=k}^{\infty} \left(\prod_{j=1}^{3} \mathcal{C}_{\ell,j} \right) \cdot (\mathbf{v}^\perp_{k,0} \quad \mathbf{v}_{k,0} \quad \mathbf{n}_{k,0})^t.$$

Despite its natural and simple definition, the corrugation matrix has intricate coefficients with integro-differential expressions. The situation is further complicated by some technicalities such as the elaborated direction field of the corrugation or the final stitching of the map used to descend to the torus.

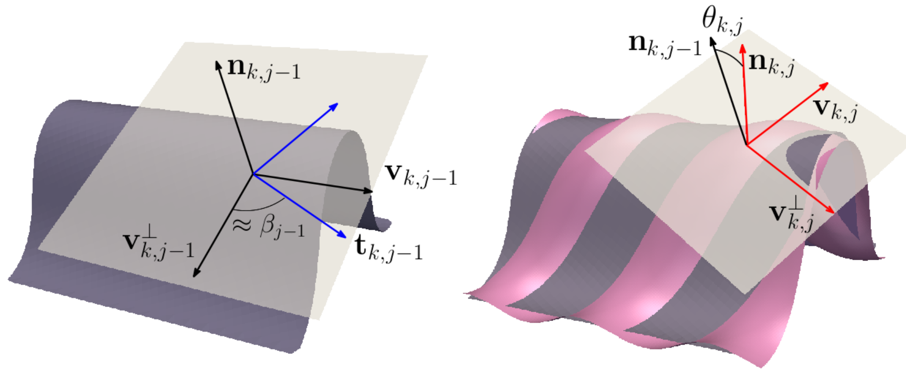

The corrugation matrix carries the frame $(\mathbf{v}^{\perp}_{k,j-1}, \mathbf{v}_{k,j-1}, \mathbf{n}_{k,j-1})$ *to* $(\mathbf{v}^{\perp}_{k,j}, \mathbf{v}_{k,j}, \mathbf{n}_{k,j})$. *The images of the maps* $f_{k,j-1}$ *and* $f_{k,j}$ *are pictured by the left gray and right pink surfaces respectively. Note that* $\mathbf{v}_{k,j} \approx \mathbf{t}_{k,j-1} \times \mathbf{n}_{k,j-1}$ *so that the intermediary frame* $(\mathbf{t}_{k,j-1}, \mathbf{n}_{k,j-1} \times \mathbf{t}_{k,j-1}, \mathbf{n}_{k,j-1})$ *is obtained by rotating* $(\mathbf{v}^{\perp}_{k,j-1}, \mathbf{v}_{k,j-1}, \mathbf{n}_{k,j-1})$ *about* $\mathbf{n}_{k,j-1}$ *by an angle approximately* β_{j-1}. *Then, the frame* $(\mathbf{v}^{\perp}_{k,j}, \mathbf{v}_{k,j}, \mathbf{n}_{k,j})$ *is approximately the rotation of the frame* $(\mathbf{t}_{k,j-1}, \mathbf{n}_{k,j-1} \times \mathbf{t}_{k,j-1}, \mathbf{n}_{k,j-1})$ *about* $\mathbf{v}_{k,j}$ *by the angle* $\theta_{k,j}$

More deeply, there is reason why things become far move involved when moving from the curves to the surfaces: the celebrated *loss of derivative phenomenon*. This loss of derivative is the major obstacle to apply a Fixed Point Theorem when trying to find a solution to the PDE of isometric maps. Let us observe where this loss of derivative phenomenon occurs in the convex integration process.

In the one dimensional setting, the convex integration process produces a new map f from an initial one f_0 by the formula:

$$f(t) := f_0(0) + \int_0^t r(u)\mathbf{e}^{i\alpha(u)\cos 2\pi N u}\,\mathrm{d}u.$$

with, as usual, $\mathbf{e}^{i\theta} := \cos\theta\,\mathbf{t} + \sin\theta\,\mathbf{n}$ and $\mathbf{t} := \frac{f_0'}{\|f_0'\|}$. We than have

$$\frac{\partial f}{\partial t}(t) = r(t)\mathbf{e}^{i\alpha(t)\cos 2\pi N t},$$

which shows that if f_0 is C^k then f is C^k also. There is no loss of derivative in that case.

In the two dimensional setting, the new map f is defined by:

$$f(t,s) := f_0(0,s) + \int_0^t r(u,s)\mathbf{e}^{i\alpha(u,s)\cos 2\pi N u}\,\mathrm{d}u + \text{gluing term}$$

where $\mathbf{e}^{i\theta} := \cos\theta\ \mathbf{t} + \sin\theta\ \mathbf{n}$, $\mathbf{t} := \frac{\partial_t f_0}{\|\partial_t f_0\|}$ and $\mathbf{n} := \frac{\partial_t f_0 \wedge \partial_s f_0}{\|\partial_t f_0 \wedge \partial_s f_0\|}$. Here, the integral over the variable t can not recover the loss of derivative due to the presence of the partial derivative $\partial_s f$ in the definition of $\mathbf{n}$. Therefore if f_0 is C^k then, generically, f is C^{k-1} only.

Fortunately, the analytic expression of the corrugation matrices considerably simplifies when considering the dominant terms of the two parts of a specific splitting of $\mathcal{C}_{k,j}$.

Corrugation Theorem (∼, S. Jabrane, F. Lazarus, B. Thibert, 2012, [1]).– *The matrix $\mathcal{C}_{k,j} \in SO(3)$ can be expressed as the product of two orthogonal matrices $\mathcal{L}_{k,j} \cdot \mathcal{R}_{k,j-1}$ where*

$$\mathcal{L}_{k,j} = \begin{pmatrix} \cos\theta_{k,j} & 0 & \sin\theta_{k,j} \\ 0 & 1 & 0 \\ -\sin\theta_{k,j} & 0 & \cos\theta_{k,j} \end{pmatrix} + O\left(\frac{1}{N_{k,j}}\right)$$

and

$$\mathcal{R}_{k,j} = \begin{pmatrix} \cos\beta_j & \sin\beta_j & 0 \\ -\sin\beta_j & \cos\beta_j & 0 \\ 0 & 0 & 1 \end{pmatrix} + O(\varepsilon_{k,j})$$

and where $\varepsilon_{k,j} := \|\langle .,. \rangle_{\mathbb{R}^2} - f_{k,j}^*\langle .,. \rangle_{\mathbb{R}^3}\|_{\mathbb{E}^2}$ is the norm of the isometric default, β_j is the angle between $V(j)$ and $V(j+1)$, and $\theta_{k,j}(p,u) = \alpha_{k,j}(p)\cos 2\pi N_{k,j} u$.

Observation.– The Corrugation Theorem gives the key to understand the infinite product defining the Gauss map. It shows that asymptotically the terms of this product resemble each other, only the amplitudes $\alpha_{k,j}$, the frequencies $N_{k,j}$ and the directions are changing. In particular, the Gauss map $\mathbf{n}_\infty$ shows an asymptotic self-similarity: the accumulation of corrugations creates a fractal structure.

Main ideas of the proof.– The matrix $\mathcal{R}_{k,j-1}$ maps $(\mathbf{v}_{k,j-1}^{\perp}\ \mathbf{v}_{k,j-1}\ \mathbf{n}_{k,j-1})$ to $(\mathbf{t}_{k,j-1}\ \mathbf{n}_{k,j-1} \times \mathbf{t}_{k,j-1}\ \mathbf{n}_{k,j-1})$ where $\mathbf{t}_{k,j-1}$ is the normalized derivative of $f_{k,j-1}$ in the direction $W_{k,j}$. This last vector field converges toward $U(j)$ when the isometric default tends to zero. Hence, $\mathcal{R}_{k,j-1}$ reduces to a rotation matrix of the tangent plane that maps $V(j-1)$ to $V(j)$. The matrix $\mathcal{L}_{k,j}$

accounts for the corrugation along the flow lines. Since $V(j) \in \ker\ \ell_j$ we have $\|df_{k,j}(V(j)) - df_{k,j-1}(V(j))\|_{\mathbb{E}^3} = O(\frac{1}{N_{k,j}})$. Therefore, modulo $O(\frac{1}{N_{k,j}})$, the transversal effect of a corrugation is not visible. In other words, a corrugation reduces at this scale to a purely one dimensional phenomenon. Hence the simple expression of the dominant part of this matrix. Notice also that the C^0-closeness of $F_{k,j}$ to $f_{k,j-1}$ implies that the perturbations induced by the stitching are not visible as well. $\square$

References

[1] V. Borrelli, S. Jabrane, F. Lazarus, B. Thibert, *Flat tori in three-dimensional space and convex integration*, PNAS 2012, vol 109, 7218-7223.

[2] S. Conti, C. De Lellis and L. Szkelyhidi, *H-principle and rigidity for $C^{1,\alpha}$-isometric embeddings*, to appear in the Proceedings of the Abel Symposium 2010, arXiv:0905.0370v1.

[3] J.-P. Kahane, Jacques Peyrière et les produits de Riesz, arXiv.org/abs/1003.4600v1.